Hovenia dulcis Fruit Peduncle Polysaccharides Reduce Intestinal Dysbiosis and Hepatic Fatty Acid Metabolism Disorders in Alcohol-Exposed Mice

Liangyu Liu , Sijie Zhu , Yuchao Zhang * , Zhenyuan Zhu , Yong Xue * , Xudong Liu *

Posted Date: 19 January 2024

doi: 10.20944/preprints202401.1447.v1

Keywords: Hovenia dulcis fruit peduncle polysaccharides; alcohol espouse; dyslipidemia; intestinal dysbiosis; hepatic fatty acid metabolism disorders

Article

Hovenia dulcis Fruit Peduncle Polysaccharides Reduce Intestinal Dysbiosis and Hepatic Fatty Acid Metabolism Disorders in Alcohol-Exposed Mice

Liangyu Liu [1,2,#], Sijie Zhu [2,3,#], Yuchao Zhang [4], Zhenyuan Zhu [3], Yong Xue [1,*] and Xudong Liu [2,*]

[1] College of Food Science and Engineering, Ocean University of China, Qingdao, China; aleliuliangyu@163.com (L.L.); xueyong@ouc.edu.cn (Y.X.)
[2] Department of Food Science and Engineering, Moutai Institute, Renhuai, China; 18798006458@163.com (S.Z.); liuxudong@mtxy.edu.cn (X.L.)
[3] College of Food Science and Engineering, Tianjin University of Science and Technology, Tianjin, China; zhyuanzhu@tust.edu.cn (Z.Z.)
[4] Department of Brewing Engineering, Moutai Institute, Renhuai, China; zyc10271027@163.com (Y.Z.)
* Correspondence: (Y.X.); liuxudong@mtxy.edu.cn (X.L.); Tel.: +86-13156204557 (Y.X.); +86-15071008384 (X.L.)
[#] These authors have contributed equally to this work

Abstract: Alcohol abuse can lead to alcoholic liver disease, becoming a major global burden. *Hovenia dulcis* fruit peduncle polysaccharides (HDPs) has the potential to alleviate alcoholic liver injury may play essential roles in treating for alcohol-exposed liver disease, however, the hepatoprotective effects and mechanisms remain unclear. In this study, the hepatoprotective effects of HDPs and its potential mechanisms were investigated in alcohol-exposed mice by liver metabolomics and gut microbiome. The results found that HDPs reduced medium-dose alcohol-caused dyslipidemia (significantly elevated T-CHO, TG, LDL-C), elevated liver glycogen levels and inhibited intestinal-hepatic inflammation (significantly decreased IL-4, IFN-γ and TNF-α), consequently reversing hepatic pathological changes. By applying gut microbiome analysis, HDPs showed significant decreases in Proteobacteria while significant increases in Firmicutes at the phylum level, and increased *Lactobacillus* abundance while decreased *Enterobacteria* abundance, maintaining the composition of gut microbiota. Further hepatic metabolomics analysis revealed that HDPs had a regulatory effect on hepatic fatty acid metabolism, by increasing the major metabolic pathways including arachidonic acid metabolism and glycerophospholipid metabolism and identified two important metabolites C00157 and C04230 involved in the above metabolism. Overall, HDPs reduced intestinal dysbiosis and hepatic fatty acid metabolism disorders in alcohol-exposed mice, suggesting that HDPs has a beneficial effect on alleviating alcohol-induced hepatic metabolic disorders.

Keywords: *Hovenia dulcis* fruit peduncle polysaccharides; alcohol espouse; dyslipidemia; intestinal dysbiosis; hepatic fatty acid metabolism disorders

1. Introduction

According to the report from World Health Organization (WHO), about 3.1 billion people with age over 15 are drinkers, and per capita consumption of alcohol can reach 32.8 g/day, exceeding the "Dietary Guidelines" for daily drinking (Chinese men or women should not consume more than 25 or 15 g/day, American men or women should not consume more than 28 or 15 g/day) [1,2]. Alcohol abuse is a global problem and is widely recognized as one of the leading causes of liver disease. Short-term acute binge drinking as well as long-term alcohol abuse can cause severe liver damage, including fatty liver, alcoholic hepatitis, liver cirrhosis and hepatocellular carcinoma [3]. Alcohol is mainly absorbed in the gastrointestinal tract, and alcohol-induced dysregulation of intestinal microecology and consequent disruption of hepatic lipid metabolism has been widely studied [4,5]. Many studies have shown that chronic alcohol abuse interferes with the intestinal microecological balance, leading to dysbiosis of the microbial community; this microecological disturbance may affect

 doi:10.20944/preprints202401.1447.v1

the intestinal barrier function and increase the infiltration of bacteria and endotoxins, thus triggering inflammatory responses and abnormalities in hepatic lipid metabolism [6,7]. In addition, alcohol abuse alters the composition and function of intestinal microorganisms, leading to disorders of hepatic lipid metabolism and increased deposition of fats in the liver; the accumulation of these fats in the liver may lead to the development of fatty liver and other liver diseases [8]. Alcohol intake can also lead to hepatocellular damage and oxidative stress, further exacerbating hepatic lipid metabolism disorders [9]. Other studies have shown that the alcohol metabolite acetaldehyde inhibits key enzyme activities in lipid metabolic pathways and interferes with the oxidative metabolism of fatty acids; such metabolic disturbances may lead to aberrant accumulation of lipids and abnormalities in lipid metabolism [10]. Overall, alcohol induces intestinal microecological disturbances and indirectly contributes to hepatic lipid metabolism disorders, which may be one of the mechanisms of alcohol damage to the liver [7,11]. However, with alcohol known to be indispensable in life, we still need to understand how it affects intestinal microecology and hepatic lipid metabolism [12]. For the prevention and treatment of alcoholic liver diseases, it is important to search for natural products with hepatoprotective effects as well as further research into the mechanisms of such protective effects.

Hovenia dulcis (known in China as Guaizao, in Japan as Japanese grape) is a traditional medicinal and edible plant in China, Korea and Japan, belonging to the Rhamnaceae family. The fruit peduncle has reddish-brown outer skin, and the fruit is sweet and more intense after frost. As a traditional herbal remedy for liver disease and alcohol poisoning, *Hovenia dulcis* has a long history in East Asia [13]. Recent studies have shown that the active ingredients in *Hovenia dulcis* have antioxidant, anti-inflammatory and anti-fibrotic properties, which can inhibit harmful substances produced during the metabolism of alcohol, and reduce damage to the liver [14–16]. However most studies are focused on *Hovenia dulcis* seeds and ignored the fruit peduncle. *Hovenia dulcis* fruit peduncle (edible fleshy part) accounts for 90% of the total fruit, which is rich in a variety of bioactive substances mainly polysaccharide, has good development and utilization value [17–19]. As the main bioactive substance in *Hovenia dulcis* fruit peduncle, *Hovenia dulcis* fruit peduncle polysaccharides (HDPs) has been proven can effectively restore the upright reflex of drinking mice, shorten sleep time and coma state [20]. Other studies suggest that acute/chronic alcoholic liver injury, non-alcoholic fatty liver disease and dyslipidemia can also be regulated by HDPs through anti-inflammatory, anti-lipid peroxidation and regulation of intestinal permeability [21,22]. In our recently study HDPs was extracted from *Hovenia dulcis* fruit peduncle and verified can effectively scavenge free radicals and inhibit biological macromolecule (protein, lipid and DNA) oxidation *in vitro* [23]. All these indicate that HDPs may play essential roles in treating for alcohol-induced liver disease, however, the underlying mechanisms involving in regulating hepatic lipid metabolism disorders largely remained elusive.

Therefore, the present study takes the HDPs obtained from *Hovenia dulcis* fruit peduncle as the object, aiming to explore the protective role of HDPs in alcohol-induced acute liver injury, and applying hepatic metabolomics combined with intestinal 16S rRNA gene sequencing analysis to gain insights into its possible mechanisms. Through this study, we hope to provide a theoretical basis for the application of HDPs in functional food and further reveal the mechanism of alcoholic liver injury.

2. Materials and Methods

2.1. Extraction and characterization of HDPs

HDPs was obtained according to the extraction method in our previous study. Briefly, the pretreatment *Hovenia dulcis* fruit peduncle was degreased, crude HDPs was prepared by water extraction and ethanol precipitation as follow conditions: solid-liquid ratio 1:25 g/mL, extraction temperature 85 °C, extraction time 1 h, ethanol precipitation volume fraction 80%. Then crude HDPs was deproteinized, decolorized and dialyzed to get the HDPs for characterization and subsequent study.

The morphology of the HDPs was observed using a scanning electronic microscope (Merlin Compact, Zeiss, Germany). The molecular weight and molecular conformation of HDPs were

 doi:10.20944/preprints202401.1447.v1

measured using Size Exclusion Chromatography-Multi-Angle Light Scattering-Refractive Index Detection (SEC-MALLS-RI), the liquid phase system was U3000 (Thermo, USA), the differential oscillometric detector was Optilab T-rEX (Wyatt technology, USA), and the laser light scattering detector was DAWN HELEOS II (Wyatt technology, USA). A gel exclusion chromatography column Ohpak SB-805 HQ (300 × 8 mm), Ohpak SB-804 HQ (300 × 8 mm) and Ohpak SB-803 HQ (300 × 8 mm) were used in series. Fourier transform infrared (FT-IR) spectra of the HDPs were determined using a spectrometer (Nicolet iZ-10, Thermo Nicolet, USA). The HDPs were mixed with KBr powder and then pressed into 1 mm pellets for FT-IR measurement in the range of 4000 to 400 cm-1. According to high-performance anion-exchange chromatography (HPAEC, ICS-5000+, Thermo Fisher, USA) on a CarboPac PA-20 anion-exchange column (3 by 150 mm, Dionex) using a pulsed amperometric detector (PAD, ICS 5000 system, Dionex) analysis, the monosaccharide composition of the HDPs is illustrated.

2.2. Animal exposure

Male C57BL/6 mice (6 weeks old, weighing about 20 g) were purchased from Hubei Animal Experimentation Center, and housed in a standard environment with constant temperature (20 ± 2) °C, constant humidity (50 ± 2) %, and light / darkness for 12 h. Mice were acclimatized for 3 days prior to the experiment. Eighty mice were randomly divided into four groups (n = 20), including control (CON) group, Low dose of alcohol (Low_ALC), Medium dose of alcohol (Medium_ALC) and HDPs + Medium dose of alcohol (HDPs_ALC). According to the per capita consumption of alcohol (32.8 g/day), the alcohol exposure dose of mice was 114 μL / 20 g after dose equivalent conversion for human and mice [24]. Consider that there is still a lot of concern about the health effects of low doses of alcohol intake, We also chose an exposure dose of 11.4 μL / 20 g. Equal amounts of distilled water were administered to the control group by gavage at regular intervals every day, and 11.4 μL / 20 g and 114 μL / 20 g of 95% edible alcohol (CAS: 20220727-Z703, production standard GB31640-2016) were administered to the mice in the Low_ALC and Medium_ALC groups at regular intervals every day, respectively. The HDPs_ALC group was administered first by gavage with 100 mg/kg HDPs for 2 h, and then 114 μL / 20 g 95% edible alcohol was administered by gavage. The treatments were continuous for 15 days. A commercial diet and filtered water were provided ad libitum. All animal studies were conducted according to the protocol approved by the Animal Care and Use Committee of Moutai Institute.

2.3. Serum biochemical analysis

The blood of mice sacrificed was centrifuged at 2000 r/min for 10 min at 4 °C, and the serum was collected. Using total cholesterol (TC, CAS: A111-1-1), triglyceride (TG, CAS: A110-1-1), low-density lipoprotein cholesterol (LDL-C, CAS: A113-1-1), and high-density lipoprotein cholesterol (HDL-C, CAS: A112-1-1) assay kits purchased from Nanjing Jiancheng Co., serum TC, TG, LDL-C and HDL-C levels were measured. The serum activities for alanine aminotransferase (ALT, CAS: C009-2-1) and aspartate aminotransferase (AST, CAS: C010-2-1) were detected by with commercial assay kits (Nanjing Jiancheng Co., Nanjing, China).

2.4. Histological examination

The fresh liver tissues of mice from each group were fixed in 4% paraformaldehyde for 24 h at room temperature, routinely dehydrated and embedded in paraffin, with a section thickness of 5 μm for hematoxylin-eosin (H&E) staining. Also, the deparaffined sections were conducted the periodic acid-schiff (PAS) staining (CAS: G1281, Solarbio) to observe glycogen changes in liver tissues [25]. These sections were scanned by a digital slide scanner (Pannoramic MIDI, 3DHISTECH, Hungary) and observed by the CaseViewer software [26].

 doi:10.20944/preprints202401.1447.v1

2.5. Biological determination of injury-related parameters in liver and intestine

Liver and intestine tissues of mice were collected to detect the levels of interleukin-4 (IL-4, CAS: H005-1-2), interferon-γ (IFN-γ, CAS: H025-1-2) and tumor necrosis factor-α (TNF-α, CAS: H052-1-2) by ELISA commercial assay kits (Nanjing Jiancheng Co., Nanjing, China). The glycogen content was detected in liver, and the levels for lipase (LPS, CAS: A054-2-1), lipopolysaccharide binding protein (LBP, CAS: A043-1-1) and α-Amylase (AMS, CAS: C016-1-1) were detected in intestine. Protein concentrations of the sample were measured with BCA protein analysis kit (Beyotime, Shanghai, China). All determinations were performed following the manufacturers' protocols.

2.6. Gut microbiota analysis

Intestines (n = 4, 3 mouse intestines pooled as one sample) were used for 16S rRNA gene amplicons sequencing. Briefly, genomic DNA was extracted from 50 mg of tissue samples and detected by 2% agarose gel electrophoresis, amplified using an ABI GeneAmp® 9700 PCR (the primer is 338F-806R). The PCR products were cut and recovered using the AxyPrepDNA gel recovery kit (AXYGEN), subsequently eluted by Tris_HCl [27]. The PCR products were quantified by QuantiFluor™ -ST Blue Fluorescence Quantification System (Promega, USA). Miseq amplicon libraries were constructed and sequenced on Illumina MiSeq-PE25 platform (Illumina, USA) in Majorbio Co. (Shanghai, China) [28]. The data were uploaded to the Majorbio Co. Cloud Platform (https://cloud.majorbio.com) for result analysis. All 16S Rrna sequence data can be downloaded from the National Center for Biotechnology Information (NCBI) under the project accession PRJNA1043446 (Submission ID: SUB13989547).

2.7. Hepatic metabolomics analysis

Livers of mice from each group (n = 4, 3 mouse livers pooled as one sample) were collected for Untargeted metabolomics [29]. Approximately 50 mg of liver tissue was added to 200 μL of water homogenate and vortexed for 60 s. 800 μL of methanol / acetonitrile (1:1) solution was vortexed for 60 s. After two times of low-temperature ultrasound (40 KHz) for 30 min, the proteins were precipitated by placing in the refrigerator at -20 °C for 1 h. The samples were centrifuged at 4 °C and 14,000 r/min for 20 min, and the supernatants were freeze-dried and stored at -80 °C. The samples were analyzed using UHPLC-ESI-Q-Exactive HF-X system (Thermo, USA). Chromatographic conditions: the column was ACQUITY UPLC HSS T3 (100 mm × 2.1 mm, 1.8 μm; Waters, Milford, USA); mobile phase A was 95% water + 5% acetonitrile (containing 0.1% formic acid), and mobile phase B was 47.5% acetonitrile + 47.5% isopropanol + 5% water (containing 0.1% formic acid); the injection volume was 3 μL, and the column temperature was 40 °C. Mass spectrometry conditions: the sample is ionized by electrospray ionization, and the mass spectrometry signals are collected in positive and negative ion scanning modes, respectively. The raw data were pre-processed by Pareto-scaling and statistically analyzed by orthogonal partial least squares discriminant analysis (OPLS-DA). The obtained metabolites were used for metabolite annotation, data processing using Progenesis QI (Waters, Milford, USA) software. Metabolites with significant differences were screened and analyzed for metabolite interactions using the software MetaboAnalyst 5.0 with conditions VIP > 1 and P < 0.05 (http://www.metaboanalyst.ca/). Metabolic pathways were constructed based on KEGG enrichment analysis (http://www.genome. jp/kegg/pathway.html). The metabolomic data have all been uploaded to Metabolights (access number MTBLS8996).

2.8. Statistical analysis

SPSS 22.0 was used to analyze the data, using one-way analysis of variance (ANOVA) and comparing mean differences between groups, with a p-value of < 0.05 indicating significance. Statistical graphs were performed using GraphPad Prism 8.0 and values were showed as mean ± standard error (Mean ± SE), except for the metabolomics analysis. Annotated metabolites were performed using multivariate statistical analysis. A principal component analysis (PCA) was first performed to inspect the data variance and were generated with a cloud platform (Majorbio Co., Shanghai). Metabolic pathway analyses were generated with MetaboAnalyst 5.0 [30]. The

Preprints (www.preprints.org) | NOT PEER-REVIEWED | Posted: 19 January 2024 doi:10.20944/preprints202401.1447.v1

significance of individual metabolites between the four treatment groups was assessed with a one-way ANOVA followed by Fisher's post hoc analysis and Holm FDR-correction, with a p -value of <0.05 indicating significance.

3. Results

3.1. Structural characterization of HDPs

The crude HDPs (Figure 1A) was purified to get the HDPs (Figure 1B) and the microstructure image of HDPs was showed in Figure 1C, the HDPs is aggregated clusters, stacked on top of each other, presenting a homogeneous porous structure, and the intermolecular morphology is tightly packed in terms of appearance and morphology, which is consistent with the molecular conformational map structure analysis (Figure 1E). The molecular weight distribution plot (Figure 1D) is based on the retention time of the assay (Time, min) as a horizontal coordinate, and the molar mass (g/mol) as a vertical coordinate; the molecular conformation plot (Figure 1E) is based on the molar mass (g/mol) as a horizontal coordinate, and the root mean square radius (R.M.S. Radius, nm) as a vertical coordinate. mol) as the horizontal coordinate and the root mean square radius (R.M.S. Radius, nm) as the vertical coordinate. The Mn value (number average molecular weight) of HDPs was calculated as 13.163 kDa, Mw value (weight average molecular weight) as 29.73 kDa, Mz value (z average molecular weight) as 134.413 kDa and Mp value (peak molecular weight) as 9.959 kDa. The slope of the graphs was -0.14±0.01, and it can be concluded that the HDPs are small molecular weight polymers and are compact and spherical. It can be inferred that HDPs are small molecular weight polymers with compact and uniform spherical conformation.

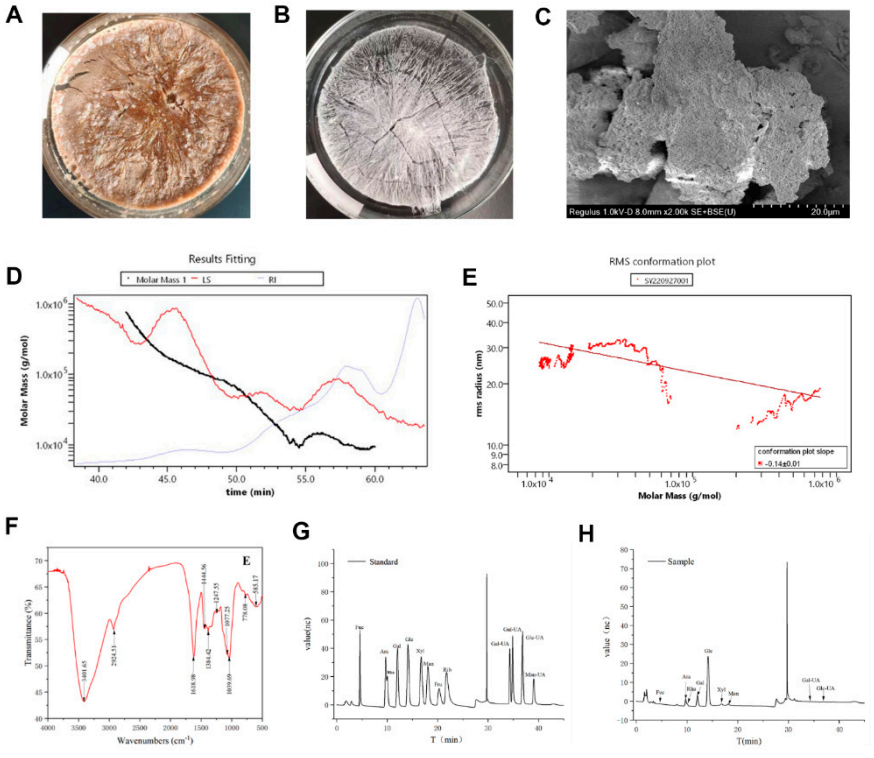

Figure 1. Structural characterization of *Hovenia dulcis* fruit peduncle polysaccharides (HDPs). (A) crude HDPs picture, (B) HDPs picture, (C) Scanning electron microscope image of HDPs, (D) Molecular weight distribution plot of HDPs, (E) Molecular conformation plot of HDPs, (F) FT-IR spectra of the HDPs, (G) Ion chromatography spectra of monosaccharide standards, (H) Ion chromatography spectra of HDPs.

As Figure 1F showed, the infrared spectrum of HDPs has typical polysaccharide characteristic bands, with a strong absorption peak at 3401.65 cm^{-1}, for the -OH stretching vibration signal peak,

Preprints (www.preprints.org) | NOT PEER-REVIEWED | Posted: 19 January 2024 doi:10.20944/preprints202401.1447.v1

and an absorption peak at 2924.51 cm^{-1} for the C-H stretching vibration signal peak, and the above two peaks are typical polysaccharide hydroxyl and alkyl groups, indicating that the sample is polysaccharide. A strong absorption peak appeared at 1,618.98 cm^{-1}, which is the stretching vibration of C=O, indicating the presence of -CHO; 1384.42~1,444.56 cm^{-1} is the C-H variable angle vibration signal peaks, and the above two peaks are also the infrared characteristic absorption peaks of polysaccharides. The band at about 1247.55 cm^{-1} shows the presence of C-O-C and C-O-H bonds. The peaks at 1039.69 cm^{-1} and 1077.25 cm^{-1} are signal peaks generated by the stretching vibration of C-O and C-C bonds in the sugar ring, respectively, which proves that the HDPs contain pyranose monosaccharides. In addition, the analysis of the monosaccharide composition shows in Figure 1G, 1H and Supplementary Table S1. The results showed that the HDPs were acidic polysaccharides and complex in structure, and their major monosaccharide components consisted of fucose, rhamnose, arabinose, galactose, glucose, Xylose, mannose, galacturonic acid, and glucuronic acid, with the following percentages (mol%): 0.55%, 11.41%, 5.15%, 14.15%, 60.66%, 2.48, 2.9%, 2.10%, and 0.62%, respectively. The content of glucuronic acid in the HDPs is very low, so its absorption peaks are not obvious in the infrared spectrogram.

3.2. Changes in serum lipid levels

The levels of serum T-CHO, TG, LDL-C, and HDL-C were higher in the Low_ALC and Medium_ALC groups of mice than in the CON group ($p < 0.05$) (Figure 2). The levels of TG, TC, and LDL-C were significantly lower ($p < 0.05$) in the HDPs group compared with the Medium_ALC group (Figure 2A-C).

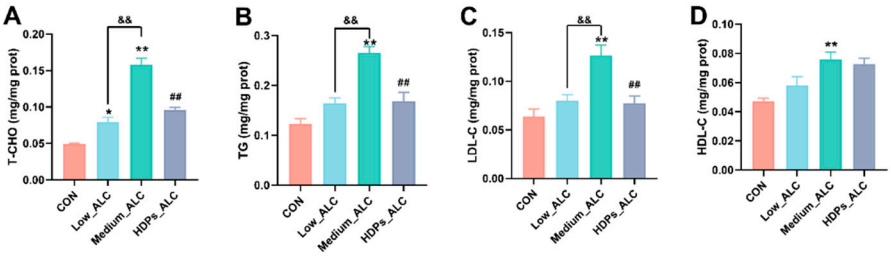

Figure 2. Effect of HDPs on serum lipid levels in alcohol-exposed mice. (A) serum T-CHO; (B) serum TG; (C) serum LDL-C; (D) serum HDL-C. *$p < 0.05$, **$p < 0.01$ compared with the CON group; &&$p < 0.01$ compared with the Low_ALC group; ##$p < 0.01$ compared with the Medium_ALC group.

3.3. Liver damage

Liver organ index, hepatic glycogen, serum ALT and AST activities were used as indicators of alcoholic acute liver function. Alcohol exposure significantly increased hepatic index, serum ALT and AST activity, decreased hepatic glycogen content and normalized after HDPs treatment compared to CON group (Figure 3A-D). Compared with the CON group, the Low_ALC and Medium_ALC groups had significant pathological changes, such as narrowing of the central vein (quantized in Supplementary Figure S1), vacuolization of hepatocytes and partial infiltration of inflammatory cells (Figure 3E), and reduction of hepatic glycogen (Figure 3F). Compared with the Medium_ALC group, the HDPs_ALC group did not show significant hepatocyte vacuolization and inflammatory cell infiltration (Figure 3Ed2).

Preprints (www.preprints.org) | NOT PEER-REVIEWED | Posted: 19 January 2024 doi:10.20944/preprints202401.1447.v1

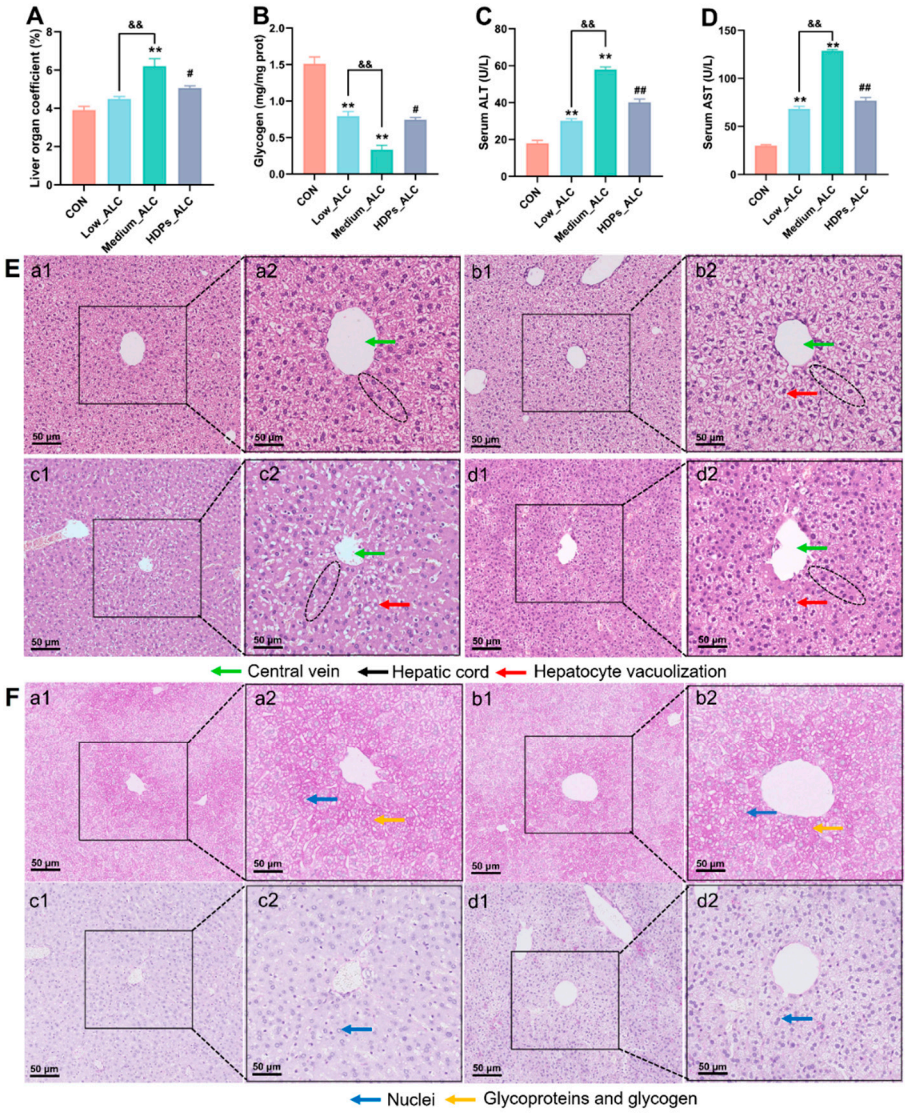

Figure 3. HDPs attenuate acute liver injury in alcohol-exposed mice. (A) Liver index, (B) hepatic glycogen, (C) serum ALT, (D) serum AST, (E) histological changes in HE-stained liver sections (bar = 50 μm), (F) histological changes in PAS-stained liver sections (Nuclei are colored blue, glycoproteins and glycogen are colored red, bar = 50 μm), a: CON, b: Low_ALC, c: Medium_ALC, d: HDPs_ALC.

3.4. Changes in hepatic and intestinal inflammatory cytokines and intestinal enzyme activities

Changes in pro-inflammatory cytokines (IL-4, IFN-γ and TNF-α) and intestinal enzyme activities in the liver and intestines of mice were measured to determine the anti-inflammatory effects of HDPs. The levels of IL-4, IFN-γ and TNF-α in the liver and intestinal tissues of mice in the Low_ALC and Medium_ALC groups were significantly higher ($p < 0.05$) compared with the CON group. These pro-inflammatory cytokines were significantly reduced ($p < 0.05$) in the HDPs_ALC group compared with the Medium_ALC group (Figure 4A, 4B). Compared with the CON group, the intestinal tissue levels of LPS and LBP were significantly higher ($p < 0.05$) and AMS levels were significantly lower ($p < 0.05$) in the Medium_ALC group. Compared with the Medium_ALC group, the levels of LPS and LBP were significantly lower ($p < 0.05$) in the HDPs_ALC group (Figure 4C).

Preprints (www.preprints.org) | NOT PEER-REVIEWED | Posted: 19 January 2024 doi:10.20944/preprints202401.1447.v1

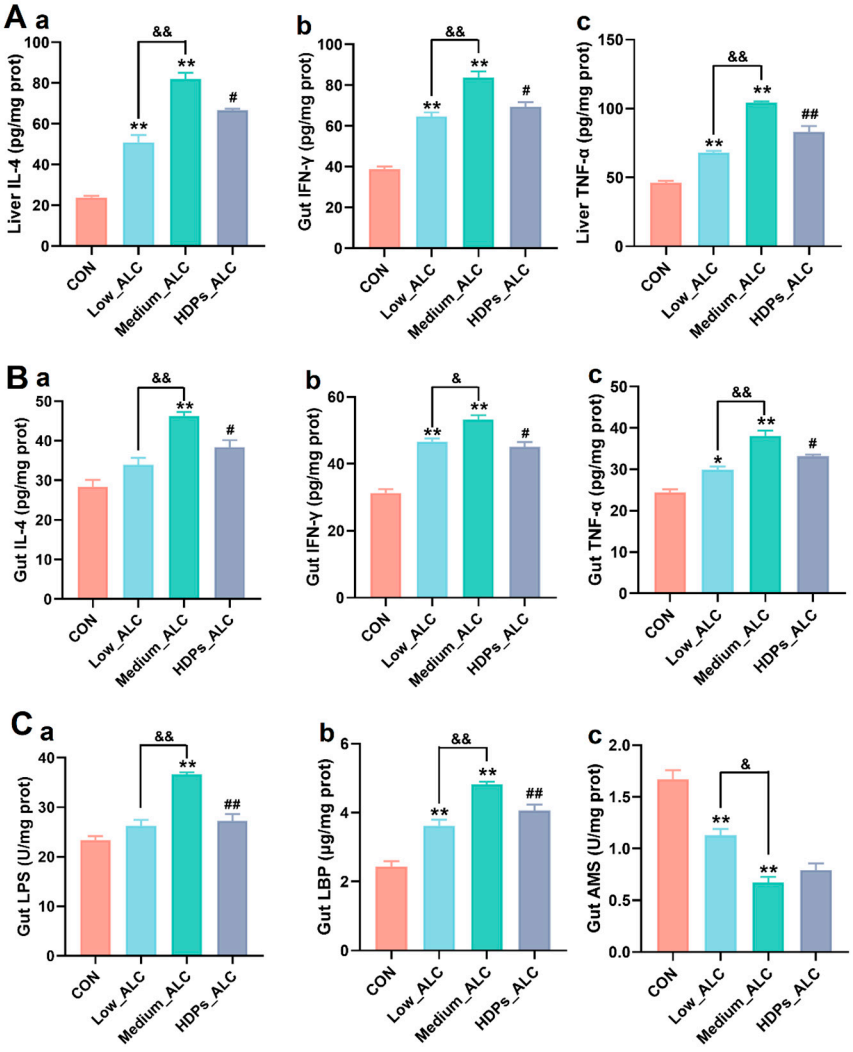

Figure 4. Effects of HDPs on hepatic and intestinal inflammatory cytokines and intestinal enzyme activities in alcohol-exposed mice. (A) Hepatitis cytokine changes, a: IL-4, b: IFN-γ, c: TNF-α; (B) intestinal inflammatory cytokine changes, a: IL-4, b: IFN-γ, c: TNF-α; (C) intestinal enzyme activity changes, a: LPS, b: LBP, c: AMS. Compared with the CON group, *p < 0.05, **p < 0.01; compared with the Low _ALC group, &p < 0.05, &&p < 0.01; compared with Medium_ALC group, #p < 0.05, ##p < 0.01.

3.5. Dysbiosis of gut microbiota

Alcohol exposure resulted in changes in the diversity, structure and composition of the gut microbiota of mice. The indices of sobs, chao and ace reflecting community richness were significantly lower in the alcohol-exposed group than in the CON group. The indices of shannon reflecting community diversity (1.55 ± 0.578) were significantly lower in the alcohol-exposed group than in the CON group (2.12 ± 0.675), while the indices of sobs, chao, ace and shannon in the HDPs_ALC group were higher compared with those in the Medium_ALC group (Supplementary Table S2). Species analysis also reflected that the gut microbiota diversity of the alcohol-exposed group was reduced (Figure 5A). Structurally, the CON and Low_ALC groups were similar in community structure and both were distributed in Quadrants I and II, while the Medium_ALC group was similar and distributed in Quadrants III and IV with the HDPs_ALC group. The CON group was clearly separated from the other groups, indicating a different community structure. HDPs_ALC group showed a crossover with both Low_ALC and Medium_ALC groups, suggesting that the HDPs_ALC group microbiota structure was somewhere in between (Figure 5B). Analysis of community composition showed that at the phylum level, the Firmicutes phylum was significantly

Preprints (www.preprints.org) | NOT PEER-REVIEWED | Posted: 19 January 2024 doi:10.20944/preprints202401.1447.v1

reduced in alcohol-exposed mice, whereas the Proteobacteria phylum was significantly increased in the high-dose alcohol group (Figure 5C). At the genus level, the *Enterobacter* genera was significantly increased in the high-dose alcohol group, while the *Dubosiella* genera was significantly reduced and the Lactobacillus genera was reduced to some extent (Figure 5D).

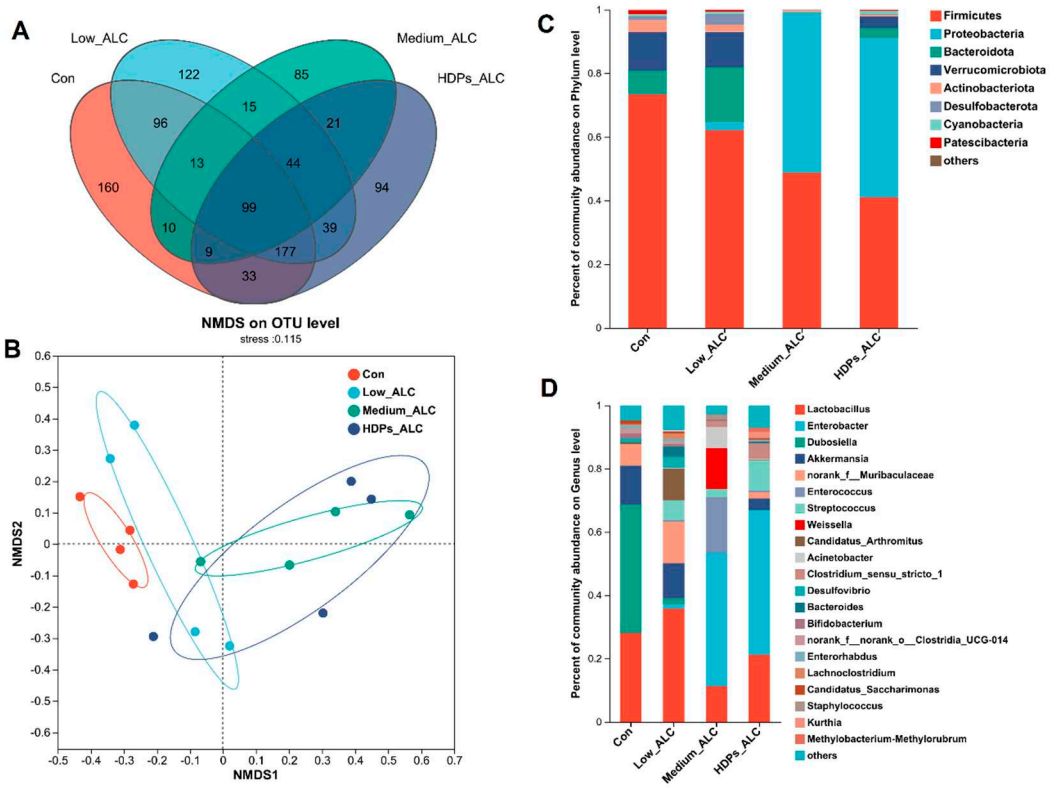

Figure 5. Differences in gut microbial community composition in alcohol-exposed mice. (A) Species Venn analysis, (B) NMDS (Nonmetric Multidimensional Scaling) analysis, (C, D) Percentage of community abundance at the phylum or genus level.

3.6. Hepatic metabolomics changes

To further understand the effects of HDPs on the metabolic response of the liver in alcohol-exposed mice, metabolic profiling of the liver was performed based on LC-MS in positive and negative ion mode. Venn, PCA and PLS-DA were used to differentiate the hepatic metabolites in different treatment groups to search for potential differential biomarkers in the liver. Venn analysis showed differences in the number of metabolites in different treatment groups, and the number of differential metabolites in the Medium_ALC group was higher than that of the CON group (Figure 6A). The PCA results showed that the principal component scores of the CON samples were very close to each other and clearly separated from the other three groups (Supplementary Figure S2). PLS-DA was applied to reveal the intervention effect of HDPs. There was obvious clustering in the Low_ALC, Medium_ALC and HDPs groups, both in positive and negative ion modes. There was a clear separation between the CON group and the alcohol-exposed group, suggesting that the liver metabolic profiles underwent obvious biochemical changes after alcohol exposure. Whereas, the HDPs group showed a better clustering tendency, which may be that the HDPs exerted an intervention effect (Figure 6B).

Preprints (www.preprints.org) | NOT PEER-REVIEWED | Posted: 19 January 2024 doi:10.20944/preprints202401.1447.v1

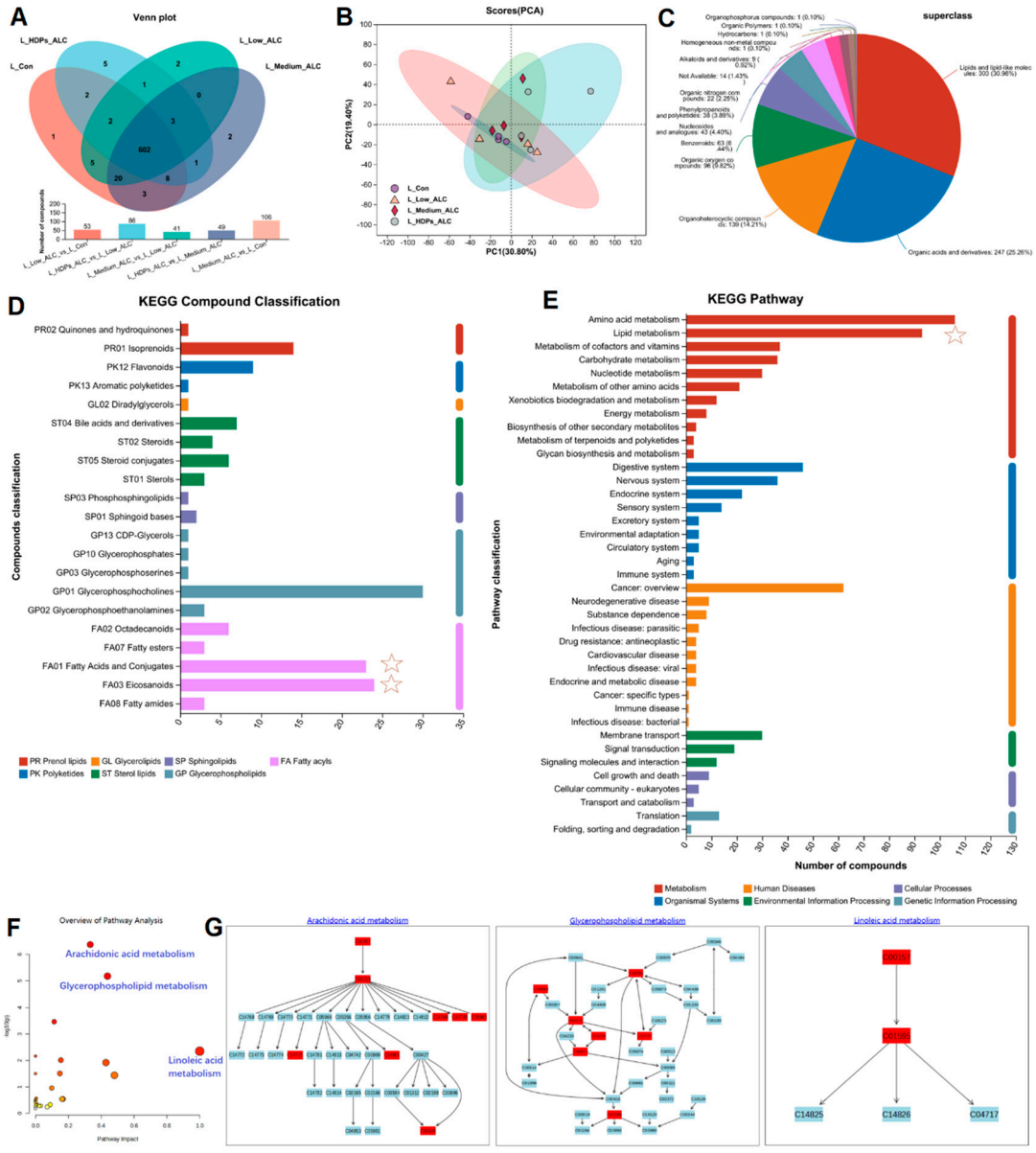

Figure 6. Changes in hepatic metabolomic profiles. (A) Metabolite Venn analysis; (B) PLS-DA analysis; (C) HMDB classification; (D) lipids KEGG classification; (E, F, G) KEGG pathway enrichment analysis.

The HMDB classification of the identified metabolites showed that the different metabolites lipids led the different treatment groups up to 303 metabolites, which accounted for 30.98% of the metabolites (Figure 6C). The volcano plot of different significant metabolites showed that the expression of some metabolites differed between control and alcohol groups (Supplementary Figure S3). A total of 285 differential metabolites were selected as potential biomarkers in the positive ion mode with VIP values above 1.0 and were significantly different between groups ($p < 0.05$). Compared with the control group, 33 metabolites were significantly up-regulated and 25 metabolites were significantly down-regulated in the Medium_ALC group. Twenty-four metabolites were significantly up-regulated and eight metabolites were significantly down-regulated in the HDPs_ALC group compared with the Medium_ALC group. Most of the differentially expressed significant metabolites could be categorized as Fatty acyls (Fatty acids and conjugates, eicosanoids), glycerophospholipids, sterol lipids, etc. (Figure 6D). KEGG-based metabolic analysis was performed to enrich the metabolic pathways of different hepatic metabolites in order to identify the important metabolic pathways affected. KEGG functional enrichment results were sequentially categorized as

Preprints (www.preprints.org) | NOT PEER-REVIEWED | Posted: 19 January 2024 doi:10.20944/preprints202401.1447.v1

Amino acid metabolism, Lipid metabolism, Metabolism of cofactors and vitamins, etc. (Figure 6E). Further analysis of Lipid metabolism by applying MetaboAnalyst revealed that the major metabolic pathways altered in the HDPs_ALC group compared to the Medium_ALC group included arachidonic acid metabolism, glycerophospholipid metabolism, and linoleic acid metabolism, meanwhile identified two important metabolites C00157 and C04230 (KEGG compounds ID, Supplementary Table S3) involved in the above metabolism (Figure 6F, G).

3.7. Correlations of lipid changes and liver metabolites with gut microbiota in alcohol-exposed mice

3.7.1. Relationship between lipid changes and gut microbiota

RDA/CCA analysis and Spearman's correlation heatmap demonstrated the correlation between alcohol-induced changes in gut microbiota composition and parameters such as serum biochemistry, hepatic inflammation. The phylum and genera in Medium_ALC group, HDPs_ALC group showed significant positive correlation with lipid-related parameters (T-CHO, TG, LDL-C, HDL-C, ALT, AST, IL-4, IFN-γ, TNF-α) (Figure 7A, C). At the phylum level, Proteobacteria were significantly and positively correlated with T-CHO (r=0.754), TG (r=0.587), LDL-C (r=0.503), HDL-C (r=0.662), ALT (r=0.653), AST (r=0.658), IL-4 (r=0.697), TNF-α (r=0.668), whereas Verrucomicrobiota, Desulfobacterota, Actinobacteriota, Bacteroidota were significantly and negatively correlated with the above parameters (Figure 7B). At the genus level, *Enterobacter* and *Enterococcus* genera were significantly and positively correlated with those parameters, whereas *Dubosiella* and *Desulfovibrio* genera were significantly and negatively correlated with those parameters (Figure 7D).

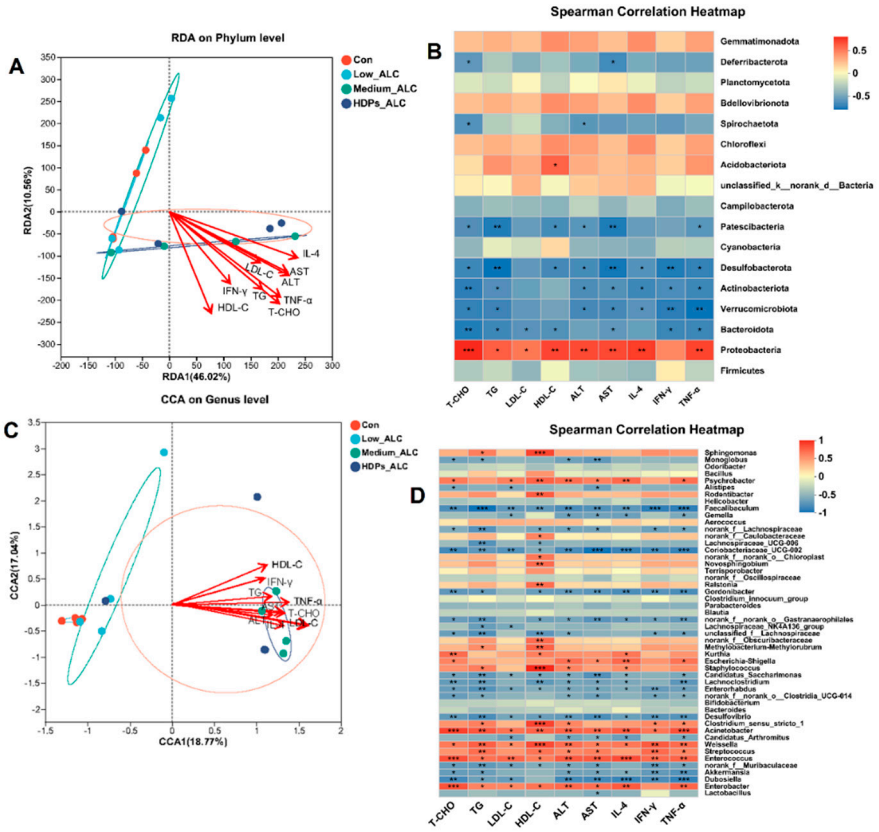

Figure 7. Spearman correlation analysis of the abundance of specific phylum genera in the intestinal flora with serum and liver parameters. (A, B) Spearman correlation analysis of the abundance of specific phylum in the intestinal flora with serum and liver parameters; (C, D) Spearman correlation analysis of the abundance of specific genus in the intestinal flora with serum and liver parameters. *p < 0.05, **p < 0.01.

Preprints (www.preprints.org) | NOT PEER-REVIEWED | Posted: 19 January 2024 doi:10.20944/preprints202401.1447.v1

3.7.2. Relationship between hepatic metabolites and gut microbiota

Spearman heatmaps visualized the relationship between gut flora and liver metabolism, and revealed strong correlations between some genera and differential hepatic metabolites (cor > 0.5 or cor < 0.5). At the phylum level, there was a positive correlation between gut flora Proteobacteria and fatty acid metabolites in the liver in alcohol-exposed group, and an increase in fatty acid metabolites in the liver was associated with an increase in the abundance of gut flora Proteobacteria (Figure 8A). At the genus level, there was a positive correlation between *Enterobacteria* genera and fatty acid metabolites of the liver in the alcohol-exposed group, and an increase in fatty acid metabolites of the liver was associated with a rise in the abundance of *Enterobacteria* genera; whereas there was a negative correlation between *Lactobacillus* genera and fatty acid metabolites of the liver (Figure 8B). After administration of HDPs treatment, C04230 metabolites in the HDPs_ALC group showed a significant decrease in Proteobacteria and a significant increase in Firmicutes at the phylum level (Figure 8C), and a significant decrease in *Enterobacter* abundance and a significant increase in *Lactobacillus* genera abundance at the genus level (Figure 8D).

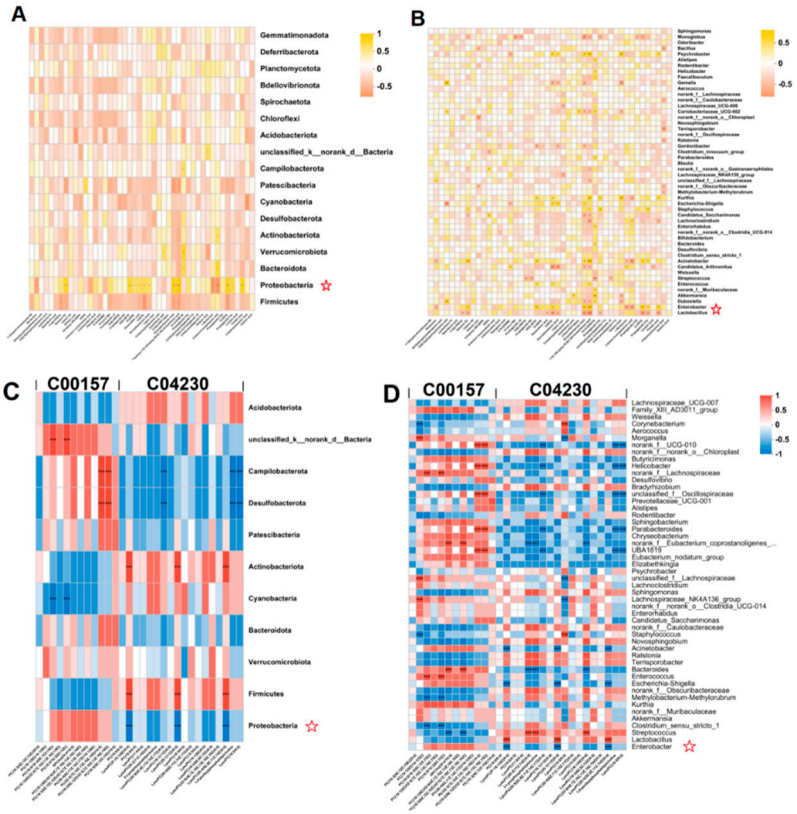

Figure 8. Positive and negative correlations of liver-identified differential metabolites with gut microbiota. (A, B) Spearman correlation heatmaps of intestinal flora in alcohol-exposed group with hepatic fatty acid metabolites at phylum and genera levels; (C, D) Spearman correlation heatmaps of intestinal flora in HDPs_ALC group at phylum and genera levels with liver-identified metabolic pathway C00157 and C04230 metabolites. *p < 0.05, **p < 0.01, ***p < 0.001.

4. Discussion

Alcohol consumption has become one of the main factors leading to liver disease. As the main natural active substance in *Hovenia dulcis* fruit peduncle, HDPs may has the potential to alleviate alcoholic liver injury. This study found that alcohol exposure can cause dyslipidemia, promote intestinal-hepatic inflammation, as well as disturb intestinal flora and lead to disruption of hepatic fatty acid metabolism, which in turn leads to pathological changes in the liver. The administration of HDPs showed a significant decrease in Proteobacteria and a significant increase in Firmicutes at the

 doi:10.20944/preprints202401.1447.v1

phylum level and increased the relative abundance of *Lactobacillus*, decreased the relative abundance of *Enterobacteria* and had a regulatory effect on fatty acid metabolism. The above suggests that HDPs maybe a potentially beneficial active ingredient for the reduce of intestinal flora and metabolic disorders caused by alcohol intake.

4.1. HDPs reduced alcohol-caused lipid abnormalities

Increasing evidence showed that alcohol consumption alters lipid metabolism [31,32]. Serum TC, TG, HDL-C and LDL-C levels are considered to be the main indicators associated with disorders of lipid metabolism. In the present study, alcohol exposure significantly elevated serum TC, TG and LDL-C levels. This is consistent with the study which displayed that the levels of serum TC and TG were significantly increased in alcohol-treated mice [33]. However, alcohol-increased the TC and TG levels returned to relatively normal levels after administration of 100 mg/kg HDPs. Changes in serum ALT and AST activities are the most intuitive biochemical parameters reflecting the degree of hepatocellular injury [34]. Alcoholic liver disease was also characterized by a significant increase in liver index [35]. The results showed that HDPs treatment significantly reduced the ALT and AST elevation caused by alcohol intake and restored the liver index to normal levels. By histological analysis of H&E, HDPs attenuated the destruction of liver lobules and the increase in hepatocyte volume after alcohol intake. Meanwhile, glycogen is the main form of energy stored in hepatocytes [36], and the alcohol-induced damaged hepatocytes in this study were unable to synthesize and store glycogen efficiently, and therefore the glycogen content was reduced. Histological results of PA-stained liver also showed that the HDPs_ALC group had normal glycogen in the liver tissues compared with the Medium_ALC group, which further confirmed the hepatoprotective effects of the HDPs.

In the alcohol-exposed group, pro-inflammatory cytokines (IL-4, IFN-γ, TNF-α) were abnormally elevated, suggesting that inflammatory were involved in the development of early alcoholic liver injury. However, there was a significant reduction in the expression of these pro-inflammatory cytokines by administration of HDPs. Consistently, the study presented that anti-steatotic and anti-inflammatory effects of *Hovenia dulcis Thumb* extracts in chronic alcohol-fed rats [21]. In addition, HDPs also reduced intestinal LPS and LBP levels and increased intestinal AMS activity. The above data fully indicate that HDPs can seem to be effective in reducing pro-inflammatory cytokines, inhibiting the intestinal inflammatory infiltration and reducing the liver inflammation induced by ingested alcohol.

4.2. HDPs alleviated alcohol-exposed intestinal dysbiosis and hepatic fatty acid metabolism disorders

Excessive alcohol consumption affects the composition of intestinal flora and microbial dysbiosis, which is considered to be the main cause of the development of alcoholic liver disease [37,38]. Furthermore, in the present study, HDPs were found to modulate the dysbiosis induced by alcohol intake. HDPs increased the sobs, chao, ace and shannon that were reduced after alcohol exposure, thereby increasing the abundance and diversity of gut microbial communities, which is important for maintaining gut health [39]. In the present study, it was found that after alcohol intake, Proteobacteria phylum increased and Firmicutes phylum decreased. This is consistent with the reported that *Antrodin A* increased Firmicutes in alcohol-exposed mice [40]. Similarly, at the genus level, alcohol intake increased the relative abundance of Enterobacter and decreased the relative abundance of *Lactobacillus* and *Dubosiella*. Lactobacillus and *Dubosiella* are mainly found in the digestive tract of mammals, and they have a variety of positive effects on the host's health, participating in the processes of food digestion and nutrient absorption, as well as in the absorption and digestion of nutrients, and may also be involved in the regulation of the immune system and host metabolism [41]. Nevertheless, certain *Enterobacter* genera are one of the common infection pathogens with multi-drug resistance that can increase intestinal infections in the host. In the present study, HDPs increased the abundance of Firmicutes and *Lactobacillus*, thus maintaining the stability of the intestinal flora composition. In addition, correlation analysis between gut microbiota and liver injury parameters showed that increased abundance of Proteobacteria phylum, *Enterobacter* genera

 doi:10.20944/preprints202401.1447.v1

was positively correlated with lipid indices and inflammatory factors, while in contrast, Firmicutes phylum, *Lactobacillus* genera were negatively correlated with lipid indices and inflammatory factors. Consequently, HDPs had an important role in lipid metabolic homeostasis by regulating hepatic lipid metabolic pathways while maintaining the stability of intestinal flora composition.

As an important organ responsible for alcohol metabolism, the liver is the main target organ for alcohol toxicity [42]. The liver plays an important role in regulating gut microbes and their actions through a variety of functions, including metabolite production and enterohepatic circulation, as well as in response to intestinal bacterial products and nutrients received through the portal vein [40]. Previous studies have shown that ethanol assumption altered intestinal barrier function and gut microbiota, leading to an increase of endotoxin release, such as LPS, that promotes a critical crosstalk between liver and gut, exacerbating steatosis, inflammation and fibrosis in liver [15]. Also, alcohol can cause alcoholic liver injury by inhibiting hepatic fatty acid metabolism and increasing hepatic lipid synthesis [9]. Hepatic metabolomics results of this study showed that alcohol exposure had the greatest negative influence on hepatic amino acid metabolism, lipid metabolism, and decreased fatty acid metabolic profiles leading to fatty acid metabolism disorders. The metabolic pathway enrichment analysis of hepatic metabolites in the HDPs_ALC group showed that, supplementation with HDPs increased arachidonic acid metabolism, glycerophospholipid metabolism, and linoleic acid metabolism. The above metabolisms are important fatty acid metabolism processes in the organism. Arachidonic acid metabolism is involved in the regulation of cell growth, immune response, inflammation and other physiological processes [43]. Glycerophospholipid metabolism involves a variety of metabolites such as phosphatidylinositol, triglycerides, phospholipids, etc., which are essential for maintaining cell membrane stability, signaling, cell proliferation and other functions [44]. Linoleic acid metabolism is mainly carried out through the triglyceride pathway and the cyclooxygenase pathway, and is involved in the regulation of blood pressure, inflammatory response and other physiological processes [45]. It can be seen that HDPs can elevated alcohol-inhibited fatty acid metabolism and maintain lipid metabolism homeostasis by regulating these pathways.

In addition, in this study, two potential biomarkers associated with Arachidonic acid metabolism were identified important metabolites C00157 and C04230 involved in the above metabolism. Furthermore, correlation analyses of intestinal flora and hepatic metabolites showed that after administration of HDPs treatment, C04230 metabolites in the HDPs_ALC group showed a significant decrease in Proteobacteria and a significant increase in Firmicutes at the phylum level, and a significant decrease in *Enterobacter* abundance and a significant increase in *Lactobacillus* genera abundance at the genus level. These potential marker genera were most likely involved in the regulation of hepatic fatty acid metabolism disorders by HDPs.

4.3. Comparison of HDPs studies

Through literature studies of HDPs and its analogs, we found these studies focused on its antioxidant activity [13], potent immunostimulatory activity [46], effects on alcoholic liver injury and alcohol metabolism [16], as well as its roles in STZ-induced type 1 diabetes mellitus [19]. Most of the studies are structural analyses, and little information on mechanisms is available, except for the hypoglycemic mechanisms of HDPs-2A (a polysaccharide purified from H. dulcis) in T1DM rats revealed by Yang et al [19]. For hepatoprotective activity *in vivo*, Wang et al [47] suggested that HDPs had significant protective effects against acute alcoholic liver injury through decreasing oxidative stress. In contrast, from the perspective of gut microbes and hepatic metabolism, this study found that HDPs reduced alcohol-caused lipid abnormalities by alleviating alcohol-exposed intestinal dysbiosis and hepatic fatty acid metabolism disorders.

5. Conclusions

In the present study, HDPs were found to reduce dyslipidemia, decrease hepatic glycogen decline, and inhibit intestinal-hepatic inflammation; on the other hand, HDPs restored the composition of gut microbiota, and effectively regulated fatty acid metabolism disorders induced by

Preprints (www.preprints.org) | NOT PEER-REVIEWED | Posted: 19 January 2024 doi:10.20944/preprints202401.1447.v1

alcohol intake, thus exerting protective effects against alcoholic liver injury. We further confirmed that the mechanism of HDPs may be related to the increase of intestinal *Lactobacillus* and decrease of *Enterobacteria*, and the increase of metabolites C00157 and C04230 involved in hepatic arachidonic acid metabolism, glycerophospholipid metabolism. These findings will provide important references for the development of natural extract polysaccharides such as HPDs, and for the prevention of alcoholic liver disease.

Given that more and more studies have now realized the potential application value of HDPs, and component resolution has changed from crude extracts to refined extracts. In terms of microbial and nutritional research that focuses on HDPs in this study, our work will start with the analysis of the gut genera and metabolic pathways that have been unearthed, and further analyze the regulatory mechanisms that improve gut health. Overall, the future research direction should be directed towards the comprehensive study of the active ingredients, pharmacological activities, clinical applications, biotechnological modifications and nutritional effects of HDPs by utilizing an integrated and multidisciplinary approach from chemical, pharmacological, clinical, biotechnological and nutritional perspectives, in order to further explore its potential medicinal and healthcare values.

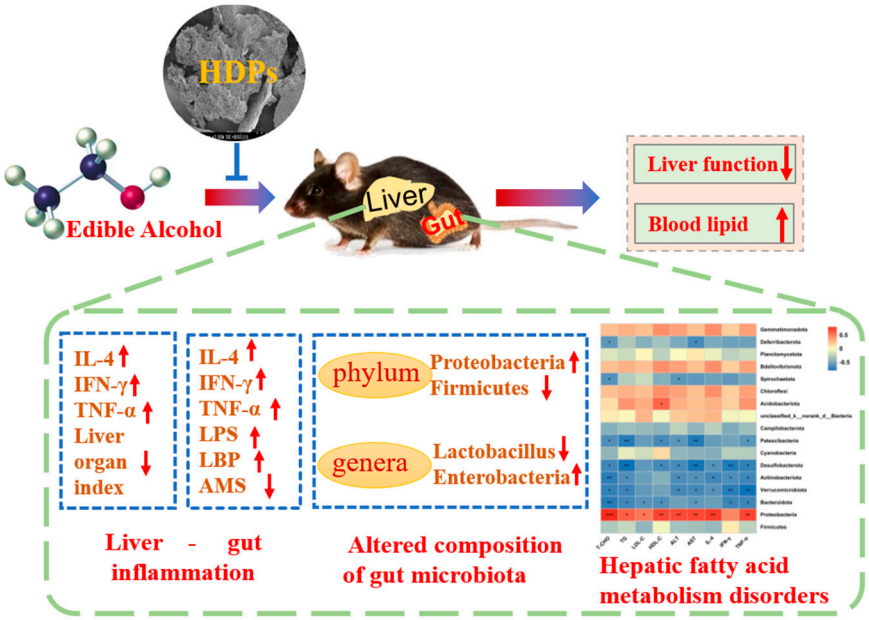

Figure 9. *Hovenia dulcis* fruit peduncle polysaccharides reduce intestinal dysbiosis and hepatic fatty acid metabolism disorders in alcohol-exposed mice. Figure 9 was originally made by Liangyu Liu and Xudong Liu.

Supplementary Materials: The following supporting information can be downloaded at the website of this paper posted on Preprints.org. Figure S1: Central vein size quantification (μm) in the liver; Figure S2: Principal component analysis (PCA) score plots visualized the results from PCA discrimination analysis; Figure S3: Volcanic map of differential metabolites in positive ion mode; Table S1: The monosaccharide composition of the HDPs (mol%); Table S2: Alpha diversity analysis; Table S3: Identified metabolites C00157 and C04230 involved in arachidonic acid metabolism, glycerophospholipid metabolism, and linoleic acid metabolism.

Author Contributions: Writing – original draft, Methodology, Validation, L.L. and S.Z. Validation, Writing – review & editing, Conceptualization, Resources, Y.Z. Writing – review & editing, Investigation, Project administration, Z.Z. Methodology, Software, Data curation, Supervision, L.L., S.Z. and Y.Z. Resources, Validation, Conceptualization, Project administration, Writing – review & editing, Y.X. and X.L. All authors have read and agreed to the published version of the manuscript.

Funding: This work was supported by the Guizhou Provincial Basic Research Program (Natural Science) (Qiankehejichu-ZK[2022]yiban541 and Qiankehejichu-ZK[2022]yiban542), Zunyi Science and Technology

projects (Zunshikehe-HZzi[2021]330 and Zunshikehe-HZzi[2022]169) and Research Foundation for Scientific Scholars of Moutai Institute (mygccrc[2022]010, mygccrc[2022]084 and mygccrc[2022]085).

Institutional Review Board Statement: The study was approved by the National Institutes of Health Guide for the Care and Use of Laboratory Animals with a certificate of Application for the Use of Animals (protocol code MI-IACUC-2022-007 and 23 May 2022 of approval).

Data Availability Statement: Data is contained within the article or Supplementary Material.

Conflicts of Interest: The authors declare no conflicts of interest. The funders had no role in the design of the study; in the collection, analyses, or interpretation of data; in the writing of the manuscript; or in the decision to publish the results.

References

1. World Health Organization. Global status report on alcohol and health 2018. World Health Organization publications: Geneva, Switzerland, 2018; pp. 38-60.
2. Zhao, C.L.; Wu, X.L.; Chen, J.; Qian, G.Q. The therapeutic effect of IL-21 combined with IFN-γ inducing CD4+CXCR5+CD57+T cells differentiation on hepatocellular carcinoma. *J Adv Res* **2021**, 36, 89–99. doi: 10.1016/j.jare.2021.05.010.
3. Liu, Y.G.; Wang J; Li, L.Z.; Hu, W.J.; Qu, Y.D.; Ding, Y.P.; Meng, L.N.; Teng, L.R.; Wang, D. Hepatoprotective Effects of Antrodia cinnamomea: The Modulation of oxidative stress signaling in a mouse model of alcohol-induced acute liver injury. *Oxid Med Cell Longev* **2017**, 7841823. doi: 10.1155/2017/7841823.
4. Avila, D.V.; Barker, D.F.; Zhang, J.; McClain, C.J.; Barve, S.; Gobejishvili, L. Dysregulation of hepatic cAMP levels via altered Pde4b expression plays a critical role in alcohol-induced steatosis. *J Pathol* **2016**, 240, 96–107. doi: 10.1002/path.4760.
5. Hartmann, P.; Hochrath, K.; Horvath, A.; Chen, P.; Seebauer, C.T.; Llorente, C., Wang, L.R.; Alnouti, Y.; Fouts, D.E.; Peter Stärkel, P.; et al. Modulation of the intestinal bile acid/farnesoid X receptor/fibroblast growth factor 15 axis improves alcoholic liver disease in mice. *Hepatology* **2018**, 67, 2150–2166. doi: 10.1002/hep.29676.
6. Chen, P.; Stärkel, P.; Turner, J.R.; Ho, S.B.; Schnabl, B. Dysbiosis-induced intestinal inflammation activates tumor necrosis factor receptor I and mediates alcoholic liver disease in mice. *Hepatology* **2015**, 61, 883–894. doi: 10.1002/hep.27489.
7. Lang, S.; Duan, Y.; Liu, J.; Torralba, M.G.; Kuelbs, C.; Ventura-Cots, M.; Abraldes, J.G.; Bosques-Padilla, F.; Verna, E.C.; Brown, R.S.J.; et al. Intestinal fungal dysbiosis and systemic immune response to fungi in patients with alcoholic hepatitis. *Hepatology*. **2020**, 71, 522–538. doi: 10.1002/hep.30832.
8. Maccioni, L.; Gao, B.; Leclercq, S.; Pirlot, B.; Horsmans, Y.; De Timary, P.; Leclercq, I.; Fouts, D.; Schnabl, B.; Stärkel, P. Intestinal permeability, microbial translocation, changes in duodenal and fecal microbiota, and their associations with alcoholic liver disease progression in humans. *Gut microbes* **2020**, 12, 1782157. doi: 10.1080/19490976.2020.1782157.
9. Li, Y.Y.; Zhong, Y.J.; Cheng, Q.; Wang, Y.Z.; Fan, Y.Y.; Yang, C.F.; Ma, Z.H.; Li, Z.H.; Li, L. miR-378b regulates insulin sensitivity by targeting insulin receptor and p110α in alcohol-induced hepatic steatosis. *Front Pharmacol* **2020**, 11, 717. doi: 10.3389/fphar.2020.00717.
10. Ambade, A.; Lowe, P.; Kodys, K.; Catalano, D.; Gyongyosi, B.; Cho, Y.; Vellve, A.I.; Adejumo, A.; Saha, B.; Calenda, C. Pharmacological inhibition of ccr2/5 signaling prevents and reverses alcohol-induced liver damage, steatosis, and inflammation in mice. *Hepatology* **2019**, 69, 1105–1121. doi: 10.1002/hep.30249.
11. Pi, A.W.; Jiang, K.; Ding, Q.C.; Lai, S.L.; Yang, W.W.; Zhu, J.Y.; Guo, R.; Fan, Y.B.; Chi, L.F.; Li, S.T. Alcohol abstinence rescues hepatic steatosis and liver injury via improving metabolic reprogramming in chronic alcohol-fed mice. *Front Pharmacol* **2021**, 12, 752148. doi: 10.3389/fphar.2021.752148.
12. Caslin, B., Mohler, K., Thiagarajan, S., Melamed, E. Alcohol as friend or foe in autoimmune diseases: a role for gut microbiome?. *Gut microbes* **2021**, 13, 1916278. doi: 10.1080/19490976.2021.1916278.
13. Yang, B.; Wu, Q.J.; Luo, Y.X.; Yang Q, Wei, X.Y., Kan, J.Q. High-pressure ultrasonic-assisted extraction of polysaccharides from Hovenia dulcis: Extraction, structure, antioxidant activity and hypoglycemic. *Int J Biol Macromol* **2019**, 137, 676–687. doi: 10.1016/j.ijbiomac.2019.07.034.
14. Qiu, P.; Dong, Y.; Zhu, T.; Luo, Y.Y.; Kang, X.J.; Pang, M.X.; Li, H.Z.; Xu, H.; Gu, C.; Pan, S.H. Semen hoveniae extract ameliorates alcohol-induced chronic liver damage in rats via modulation of the abnormalities of gut-liver axis. *Phytomedicine* **2019**, 52, 40–50. doi: 10.1016/j.phymed.2018.09.209.

15. Sferrazza, G.; Brusotti, G.; Zonfrillo, M.; Temporini, C.; Tengattini, S.; Bononi, M.; Tateo, F.; Calleri, E.; Pierimarchi, P. Hovenia dulcis Thumberg: Phytochemistry, pharmacology, toxicology and regulatory framework for its use in the European Union. *Molecules* **2021**, 26, 903. doi: 10.3390/molecules26040903.
16. Meng, X.; Tang, G.Y.; Zhao, C.N.; Liu, Q.; Xu, X.Y.; Cao, S.Y. Hepatoprotective effects of Hovenia dulcis seeds against alcoholic liver injury and related mechanisms investigated via network pharmacology. *World J Gastroenterol* **2020**, 26, 3432–3446. doi: 10.3748/wjg.v26.i24.3432.
17. Hyun, T.K.; Eom, S.H.; Yu, C.Y.; Roitsch, T. Hovenia dulcis--an Asian traditional herb. *Planta Med* **2010**, 76, 943-949. doi: 10.1055/s-0030-1249776.
18. Yang, B.; Luo, Y.X.; Sang, Y.X.; Kan, J.Q. Isolation, purification, structural characterization, and hypoglycemic activity assessment of polysaccharides from Hovenia dulcis (Guai Zao). *Int J Biol Macromol* **2022**, 208, 1106–1115. doi: 10.1016/j.ijbiomac.2022.03.211.
19. Yang, B.; Luo, Y.X.; Wei, X.Y.; Kan, J.Q. Polysaccharide from Hovenia dulcis (Guaizao) improves pancreatic injury and regulates liver glycometabolism to alleviate STZ-induced type 1 diabetes mellitus in rats. *Int J Biol Macromol* **2022**, 214, 655–663. doi: 10.1016/j.ijbiomac.2022.06.147.
20. Tang, H.H.; Zhu, S.L. Research progress of Hovenia dulcis' antialcoholism and liver protection effect. *Food and Nutrition in China* **2012**, 18, 69–72. doi: 10.3969/j.issn.1006-9577.2012.02.019 (in Chinese with English abstract).
21. Choi, R.Y.; Woo, M.J.; Ham, J.R.; Lee, M.K. Anti-steatotic and anti-inflammatory effects of Hovenia dulcis Thunb extracts in chronic alcohol-fed rats. *Biomed Pharmacother* **2017**, 90, 393–401. doi: 10.1016/j.biopha.2017.03.077.
22. Liu, Y.; Qiang, M.L.; Sun, Z.G.; Du, Y.Q. Optimization of ultrasonic extraction of polysaccharides from Hovenia dulcis peduncles and their antioxidant potential. *Int J Biol Macromol* **2015**, 80, 350-357. doi: 10.1016/j.ijbiomac.2015.06.054.
23. Liu, X.D.; Zhang, Y.C.; Zhu, S.J.; Song, Y.; Zhang, Z.H.; Chen, G.X. Optimization of extraction process of polysaccharides from Hovenia dulcis fruit pedicels and its antioxidant activity. *Science and Technology of Food Industry* **2023**, 44, 230-237. doi: 10.13386/j.issn1002-0306.2022090032 (in Chinese with English abstract).
24. Li, C. Replication of Animal Models for Human Diseases. People's Medical Publishing House: Beijing, China, 2008; pp. 60-62.
25. Wong, H.L.X.; Qin, H.Y.; Tsang, S.W.; Zuo, X.; Che, S.; Chow, C.F.W.; Li, X.; Xiao, H.T.; Zhao, L.; Huang, T. Early life stress disrupts intestinal homeostasis via NGF-TrkA signaling. *Nat Commun* **2019**, 10, 1745. doi: 10.1038/s41467-019-09744-3.
26. Chen, X.; Li, H.D.; Bu, F.T.; Li, X.F.; Chen, Y.; Zhu, S.; Wang, J.N.; Chen, S.Y.; Sun, Y.Y.; Pan, X.Y.; et al. Circular RNA circFBXW4 suppresses hepatic fibrosis via targeting the miR-18b-3p/FBXW7 axis. *Theranostics* **2020**, 10, 4851–4870. doi: 10.7150/thno.42423.
27. Zhang, Y.; Jia, X.B.; Liu, Y.C.; Yu, W.Q.; Si, Y.H.; Guo, S.D. Fenofibrate enhances lipid deposition via modulating PPARγ, SREBP-1c, and gut microbiota in ob/ob mice fed a high-fat diet. *Front Nutr* **2020**, 9, 971581. doi: 10.3389/fnut.2022.971581.
28. Han, H.; Wang, M.Y.; Zhong, R.Q.; Yi, B.; Schroyen, M.; Zhang, H.F. Depletion of gut microbiota inhibits hepatic lipid accumulation in high-fat diet-fed mice. *Int J Mol Sci* **2022**, 23, 9350-9371. doi: 10.3390/ijms23169350.
29. Lu, X.R.; Ma, N.; Liu, X.W.; Li, S.H.; Qin, Z.; Bai, L.X.; Yang, Y.J.; Li, J.Y. Untargeted and targeted metabolomics reveal the underlying mechanism of aspirin eugenol ester ameliorating rat hyperlipidemia via inhibiting fxr to induce cyp7a1. *Front Pharmacol* **2021**,12, 733789. doi: 10.3389/fphar.2021.733789.
30. Xia, J.; Wishart, D.S. Using MetaboAnalyst 3.0 for comprehensive metabolomics data analysis. *Curr Protoc Bioinformatics* **2016**, 55, 11–14. doi: 10.1002/cpbi.11.
31. Arab, J.P.; Cabrera, D.; Sehrawat, T.S.; Jalan-Sakrikar, N.; Verma, V.K.; Simonetto, D.; Cao, S.; Yaqoob, U.; Leon, J.; Freire, M. Hepatic stellate cell activation promotes alcohol-induced steatohepatitis through Igfbp3 and SerpinA12. *J Hepatol* **2020**, 73, 149–160. doi: 10.1016/j.jhep.2020.02.005.
32. Clugston, R.D.; Huang, L.S.; Blaner, W.S. Chronic alcohol consumption has a biphasic effect on hepatic retinoid loss. *FASEB J* **2015**, 29, 3654–3667. doi: 10.1096/fj.14-266296.
33. Yang. C.; Liao, A.M.; Cui, Y.; Yu, G.; Hou, Y.; Pan, L.; Chen, W.J.; Zheng, S.N.; Li, X.X.; Ma, J.R.; et al. Wheat embryo globulin protects against acute alcohol-induced liver injury in mice. *Food Chem Toxicol* **2021**, 153, 112240. doi: 10.1016/j.fct.2021.112240.

34. Zhao, J.; Zhang, S.L.; You, S.P.; Liu, T.; Xu, F.; Ji, T.F.; Gu, Z.Y. Hepatoprotective effects of nicotiflorin from nymphaea candida against concanavalin a-induced and d-galactosamine-induced liver injury in mice. *Int J Mol Sci* **2017**, 18, 587. doi: 10.3390/ijms18030587.
35. Gu, C.W.; Zhou, Z.H.; Yu, Z.H.; He, M.L.; He, L.Q.; Luo, Z.A.; Xiao, W.D.; Yang, Q.; Zhao, F.F.; Li, L.H.; et al. The microbiota and it's correlation with metabolites in the gut of mice with nonalcoholic fatty liver disease. *Front Cell Infect Microbiol* **2022**, 12, 870785. doi: 10.3389/fcimb.2022.870785.
36. Frandsen, H.S.; Vej-Nielsen, J.M.; Smith, L.E.; Sun, L.; Mikkelsen, K.L.; Thulesen, A.P.; Hagensen, C.E.; Yang, F.Q.; Rogowska-Wrzesinska, A. Mapping proteome and lipidome changes in early-onset non-alcoholic fatty liver disease using hepatic 3d spheroids. *Cells* **2022**, 11, 3216. doi: 10.3390/cells11203216.
37. Samuelson, D.R.; Shellito, J.E.; Maffei, V.J.; Tague, E.D.; Campagna, S.R.; Blanchard, E.E.; Luo, M.; Taylor, C.M.; Ronis, M.J.J.; Molina, P.E.; et al. Alcohol-associated intestinal dysbiosis impairs pulmonary host defense against Klebsiella pneumoniae. *PLoS Pathog* **2017**, 13, e1006426. doi: 10.1371/journal.ppat.1006426.
38. Duan, Y.; Chu, H.K.; Brandl, K.; Jiang, L.; Zeng, S.L.; Meshgin, N.; Papachristoforou, E.; Argemi, J.; Mendes, B.G.; Wang, Y.H.; et al. CRIg on liver macrophages clears pathobionts and protects against alcoholic liver disease. *Nat Commun* **2021**, 12, 7172. doi: 10.1038/s41467-021-27385-3.
39. Deng, L.; Wojciech, L.; Png, C.W.; Koh, E.Y.; Aung, T.T.; Kioh, D.Y.Q.; Chan, E.C.Y.; Malleret, B.; Zhang, Y.L.; Peng, G.N.; et al. Experimental colonization with Blastocystis ST4 is associated with protective immune responses and modulation of gut microbiome in a DSS-induced colitis mouse model. *Cell Mol Life Sci* **2022**, 79, 245. doi: 10.1007/s00018-022-04271-9.
40. Yi, Z.W.; Liu, X.F.; Liang, L.H.; Wang, G.Q.; Xiong, Z.Q.; Zhang, H.; Song, X.; Ai, L.Z.; Xia, Y.J. Antrodin a from antrodia camphorata modulates the gut microbiome and liver metabolome in mice exposed to acute alcohol intake. *Food Funct* **2021**, 12, 2925–2937. doi: 10.1039/d0fo03345f.
41. Zhu, S.L.; Wu, Y.Z.; Ye, X.L.; Ma, L.; Qi, J.Y.; Yu, D.; Wei, Y.Q.; Lin, G.G.; Ren, G.P.; Li, D.S. FGF21 ameliorates nonalcoholic fatty liver disease by inducing autophagy. *Mol Cell Biochem* **2016**, 420, 107-119. doi: 10.1007/s11010-016-2774-2.
42. Qu, J.L.; Chen, Q.Y.; Wei, T.F.; Dou, N.; Shang, D.; Yuan, D. Systematic characterization of Puerariae Flos metabolites in vivo and assessment of its protective mechanisms against alcoholic liver injury in a rat model. *Front Pharmacol* **2022**, 13, 915535. doi: 10.3389/fphar.2022.915535.
43. Bartel, J.; Krumsiek, J.; Schramm, K.; Adamski, J.; Gieger, C.; Herder, C.; Carstensen, M.; Peters, A.; Rathmann, W.; Roden, M.; et al. The human blood metabolome-transcriptome interface. *PLoS Genet* **2015**, 11: e1005274. doi: 10.1371/journal.pgen.1005274.
44. Zhu, Y.; Wei, Y.L.; Karras, I.; Cai, P.J.; Xiao, Y.H.; Jia, C.L.; Qian, X.L.; Zhu, S.Y.; Zheng, L.J.; Hu, X.; et al. Modulation of the gut microbiota and lipidomic profiles by black chokeberry (Aronia melanocarpa L.) polyphenols via the glycerophospholipid metabolism signaling pathway. *Front Nutr* **2022**, 9, 913729. doi: 10.3389/fnut.2022.913729.
45. Du, L.J.; Wang, Q.; Ji, S.; Sun, Y.F.; Huang, W.J.; Zhang, Y.P.; Li S.S.; Yan, S.K.; Jin, H.Z. Metabolomic and microbial remodeling by shanmei capsule improves hyperlipidemia in high fat food-induced mice. *Front Cell Infect Microbiol* **2022**, 12, 729940. doi: 10.3389/fcimb.2022.729940.
46. Niiya, M.; Shimato, Y.; Ohno, T.; Makino, T. Effects of Hovenia dulcis fruit and peduncle extract on alcohol metabolism. *J Ethnopharmacol* **2023**, 321: 117541. doi: 10.1016/j.jep.2023.117541.
47. Wang, M.C.; Zhu, P.L.; Jiang, C.X.; Ma, L.P.; Zhang, Z.J.; Zeng, X.X. Preliminary characterization, antioxidant activity in vitro and hepatoprotective effect on acute alcohol-induced liver injury in mice of polysaccharides from the peduncles of Hovenia dulcis. *Food Chem Toxicol* **2012**, 50, 2964-2970. doi: 10.1016/j.fct.2012.06.034.